Cell Communication and Signaling

RESEARCH

Open Access

Inclusion of AVβ3 integrin into extracellular vesicles in a caveolin-1 tyrosine-14-phosphorylation dependent manner and subsequent transfer to recipient melanoma cells promotes migration, invasion and metastasis

R. Huilcaman[1,2,9†], A. Campos[1,2,8†], P. Contreras[1], L. Simón[1,2,3], M. Varas-Godoy[2,4,5], F. Grünenwald[6], Baohai Shao[7], Jay Heinecke[7], L. Lobos-Gonzalez[1,2], L. Leyton[1,2*] and A. F. G. Quest[1,2*]

Abstract

Caveolin-1 (CAV1) is a membrane protein that promotes migration, invasion and metastasis of cancer cells when phosphorylated on tyrosine-14 (Y14) by a cell intrinsic mechanism involving the activation of a novel Rab5-Rac1 signaling axis. Moreover, CAV1 expressed in aggressive cancer cells is included into extracellular vesicles (EVs) and such EVs increase the metastatic potential of recipient lower grade cancer cells. However, the relevance of CAV1 Y14 phosphorylation in these extrinsic EV-stimulated events remained to be determined. Here we used B16F10 mouse melanoma cells over-expressing wild-type CAV1, phospho-mimetic CAV1(Y14E) or phospho-null CAV1(Y14F) as models to determine how the EV protein content was affected by Y14 phosphorylation and how these EVs modulated the metastatic potential of recipient B16F10 cells lacking CAV1. EVs from B16F10 cells over-expressing wild-type and CAV1(Y14/E) contain CAV1, and other proteins linked to signaling pathways associated with cell adhesion and migration. CAV1 inclusion in EVs was reduced by the Y14F mutation and global protein composition was also significantly different. Moreover, CAV1 wild-type and CAV1(Y14E) EVs promoted migration, as well as invasion of cells lacking CAV1 [B16F10(Mock) cells]. In addition, β3 integrin was transferred via CAV1(Y14E) EVs to B16F10 (Mock) cells, and treatment with such EVs promoted metastasis of recipient B16F10(Mock) cells. Finally, CAV1(Y14E) EV-enhanced migration, invasion and metastasis of recipient cells was blocked by anti-αVβ3 antibodies. In conclusion, CAV1 phosphorylated on Y14 not only intrinsically promotes migration, invasion and metastasis of

†R. Huilcaman and A. Campos contributed equally to this work.

*Correspondence:
L. Leyton
lleyton@med.uchile.cl
A. F. G. Quest
aquest@med.uchile.cl

Full list of author information is available at the end of the article

cells expressing the protein (*in cis*), but also favors the inclusion of CAV1 into EVs, as well as the extrinsic acquisition of malignant traits in recipient cells, through integrin transfer (*in trans*).

Keywords Exosomes, Caveolin-1, B16F10 cells, Integrin transfer, Cancer malignancy

Introduction

Cancer is the second leading cause of death from non-communicable disease after cardiovascular diseases [1]. Approximately, 10 million people die annually from cancer and 19.3 million new cases are diagnosed every year, according to recent data [2]. Melanoma is considered one of the most common cancers and its global incidence has risen significantly over the last few decades. This type of neoplasm is characterized by increased mortality rates due to early onset of metastasis and increased development of resistance to chemotherapeutic drugs used to treat these patients [3, 4]. For tumor cells to metastasize, they must acquire specific traits, including increased adhesion, migration and invasiveness, which favour intravasation, as well as extravasation once reaching the target tissue and formation of a secondary tumor [5, 6]. Intriguingly, several of these events are known to be promoted by Caveolin-1 (CAV1), an integral membrane and scaffolding protein which is upregulated in advanced cancer patients with melanoma, breast, prostate and colon cancer [7–9]. Previous reports from our group evaluated the pro-metastatic role of CAV1 using the murine melanoma cell line B16F10, which lacks CAV1. In addition, overexpression of CAV1, observed after transfection of B16F10 cells, leads to increased cell migration and invasion via activation of a novel CAV1-Rab5-Rac1 signalling axis [10, 11]. Interestingly, the overexpression of CAV1 also enhanced lung metastasis upon injection of these cells into the tail vein of C57BL/6 mice [12]. Moreover, CAV1 phosphorylation on tyrosine 14 (Y14) enhances migration in a manner dependent on the extracellular matrix [13]. Substrates found in the lung, such as fibronectin, enhance persistency and directionality of migration, which ultimately translates into increased metastasis in an in vivo model using C57BL/6 mice. Furthermore, this ability was shown to depend on phosphorylation of CAV1 on Y14 [13, 14]. However, whether CAV1 promotes metastasis solely via mechanisms involving signalling within the same cell (intrinsically, *in cis*) or also between cells (extrinsically, *in trans*) is a relevant issue [15], especially bearing in mind that the metastatic process itself is rather inefficient [16–18].

Extracellular vesicles (EVs) are membrane-enclosed and ceramide-enriched vesicles that are secreted by a wide variety of mammalian, as well as prokaryotic cells [19]. Most notably, they are widely implicated in processes favouring cancer development and progression [20]. These vesicles are known to transport a variety of biomolecules, including proteins, nucleic acids, and lipids, and, importantly in the context of metastasis, are capable of modifying the biological behaviour of adjacent or distant recipient cells [21, 22]. EVs can be roughly divided into two major categories, exosomes and microvesicles, according to their biogenesis [21, 23]. Interestingly, CAV1 has been detected in prostate cancer-derived EVs, known to enhance tumor formation in in vitro and in vivo models [24, 25]. Furthermore, CAV1 expression is upregulated in murine melanoma models and in melanoma patients when compared to healthy controls and is also detected in EVs isolated from melanoma patient blood samples [12, 26–28].

Indeed, recent studies from our laboratory have shown that CAV1 is a component of EVs released by metastatic human breast cancer cells that promote migration and invasion of less aggressive recipient cells in a CAV1-dependent manner [29]. These CAV1-containing EVs were shown to include a unique set of adhesion-related proteins that could explain how the vesicles promote the acquisition of more aggressive traits in recipient cells [29, 30]. Beyond the global effect of CAV1 on EV composition, it also became important to determine whether the phosphorylation on Y14 was relevant in this context. Thus, in the present study, B16F10 cells expressing or not CAV1 wild-type or Y14 mutant proteins were used to determine how the EV protein content was affected by Y14 phosphorylation and how these vesicles modulated the behaviour of recipient B16F10 cells lacking CAV1.

Methods

Cell lines

B16F10 cells were transfected with pLacIOP to overexpress CAV1, CAV1(Y14E), or CAV1(Y14F) induced by IPTG (US Biological Cat. 1850) [13]. Transfected cells were selected with 750 µg/mL hygromycin B (US Biological. Cat. H9700-05B). Cells were cultured in RPMI 1640 (Gibco. Cat. 23400-021) supplemented with 5% fetal bovine serum (FBS, Biological Industries. Cat. 040011 A) EV-free and 1% penicillin/streptomycin (Gibco. Cat. 15640-055) at 37 °C and 5% CO2.

EV-free serum preparation

Fetal bovine serum (Biological Industries. Cat. 040011 A) was ultracentrifuged at 100.000x*g* for 16 h at 4 °C. A T-1250 rotor was used in a Thermo Fisher Scientific Sorvall ultracentrifuge [29, 30].

EV isolation

Cells were allowed to proliferate until they reached 70–80% confluency in 100 mm plates and conditioned media were collected. Supernatants were centrifuged at 300x*g* for 10 min to eliminate cells, 2000x*g* for 30 min and 10,000x*g* for 40 min to eliminate cell debris and larger vesicles. Finally, supernatants were centrifuged at 100,000x*g* for 90 min at 4 °C. EV pellets were resuspended in 1 mL PBS and centrifuged again at 100,000x*g* for 90 min at 4 °C. Resulting pellets were resuspended in 200 µL PBS. For these experiments T-1250 and TH-641 rotors were used in a Thermo Fisher Scientific Sorvall ultracentrifuge.

Nanoparticle tracking analysis

The concentration and size of EVs (diluted 1:1000 to 1:100 in PBS) were analyzed using the NanoSight NS300 instrument (NanoSight NTA 3.2 Dev Build 3.2.16, NanoSight Ltd). Measurements were conducted using a 532-nm laser, with the camera set to level 9 and the detection threshold at 5 (Camera sCMOS). For each preparation, the camera recorded three videos, each lasting 30 s. These videos were subsequently analyzed to determine the average and mode of the particle sizes in each sample, along with an estimate of the total number of particles present.

Transmission electron microscopy

EV samples (5 µL) were placed on copper grids coated with formvar (Sigma. Cat. TEM-FCF200NI50). After drying, 15 µL of uracil acetate was added for 1 min. Images were obtained using a Talos F200C G2 microscope (Thermo Fisher Scientific, Facultad de Ciencias Biologicas, Pontificia Universidad Catolica de Chile).

Western blotting

Cells were rinsed in ice-cold PBS containing 1 mM orthovanadate, 10 µg/mL benzamidine, 10 µg/mL antipain, 12.5 µg/mL leupeptin, 1 mM phenylmethyl-sulphonyl fluoride (OVA-BAL-PMSF), and 10 mM NaF. Then, cells were harvested in lysis extraction buffer (HEPES 0.2 mM pH 7.4, and SDS 10% plus OVA-BAL-PMSF, Thermo fisher). EV samples (40 µL) were diluted with 10 µL lysis extraction buffer and sonicated. After sonication, protein concentrations in extracts were determined using the BCA protein assay kit (Thermo Scientific. Cat. 23225). Protein samples were separated by SDS-PAGE (15 µg per lane), transferred to nitrocellulose, blocked in PBS containing 5% non-fat milk and probed overnight at 4°C with the primary antibodies against Alix (Santa Cruz, 1:3000, sc-53540), CD81 (Santa Cruz, 1:3000, sc-166029), TSG101 (Santa Cruz, 1:3000, sc-7964), CAV1 (Transduction Lab, 1:1000 610407), ITGB3 (Merck, 1:3000, AB2984) diluted in 5% non-fat milk containing 0.1% Tween-20. Protein loading in each lane was assessed by probing with an anti-β-actin antibody (Sigma-Aldrich, 1:5000, A5316). Goat anti-rabbit (Rockland, 1:5000, 611–1302) or anti-mouse (Rocklan, 1:5000, 610–4302) IgG antibodies coupled to horseradish peroxidase were used to detect bound primary antibodies by EZ-ECL. Protein bands were quantified by densitometric analysis using the ImageJ 1.52a software (available from NIH at https://imagej.nih.gov).

Cell pre-treatment with EVs

B16F10(Mock) cells (3×10^5) were cultured in 6 mm plates for 24 h. The medium was replaced by RPMI supplemented with 5% EV-free FBS. Cells were treated with EVs (10 µg) for 24 h.

For the EV functionality assays, EVs (10 µg) were pre-treated with anti-αVβ3 (Abcam, 2 µg/mL, ab78289) or anti-β1 (Santa Cruz, 2 µg/mL, sc-7312) antibody for 30 min at 37 °C. Then, EVs were incubated with cells at 37 °C for 24 h. Finally, cells were used for subsequent migration, invasion, or metastasis assays.

Migration and invasion assays

Cell migration was evaluated in Boyden Chamber assays (Transwell Costar, 6.5-mm diameter, 8-mm pore size), whereas invasion was evaluated in Matrigel assays (BD Biosciences, 354480), as reported previously [12, 29, 30].

Metastasis assays

This study was performed according to the rules and standards established by the Bioethics Committee on Animal Research in the Faculty of Medicine, University of Chile (CBA 1169 FMUCH, year of approval: 2021). Briefly, C57BL/6 mice between 8 and 12 weeks of age were subdivided randomly into different groups. These groups received an intravenous injection into the tail vein of 2×10^5 B16-F10 cells, pre-treated with 1mM IPTG for 48 h (CAV1 induction), and EVs for 24 h. Mice were euthanized on day 21 post-injection, and the lungs were removed and fixed in Fekete's solution (70% ethanol, 10% formalin, and 5% glacial acetic acid). Tumour nodules were separated from the lung parenchyma and weighed. Metastasis is expressed as black tissue mass/total lung mass (%) [12, 13, 31].

EV uptake

EVs were labelled with PKH67 (Green Fluorescent Linker Midi Kit for General Cell Membrane. Sigma Aldrich. Cat. PKH67GL). After 5 min, EVs were separated in Exo-spin columns according to the manufacturer's instructions. B16F10(Mock) cells (5×10^4) were seeded in 24 well-plates for 24 h. Then, the medium was replaced by RPMI with 5% EV-free FBS. EVs labelled with PKH67 (1000, 3000, or 5000 EVs) were added to cells for 3–24 h. Cells

were then harvested, rinsed, and resuspended in PBS for flow cytometry analysis (BD FACS Canto cytometer).

Sample preparation for proteomics analysis

Proteins were extracted from EVs isolated from conditioned media and prepared for MS/MS analysis. EV samples (10 µg) were diluted in sodium deoxycholate (3%) and ammonium bicarbonate (NH_4HCO_3 100 mM) to yield a total volume of 55 µL per sample. The samples were then treated with dithiothreitol (DTT, 100 nM, 5 µL) to denature the proteins, placed on a heating block for 30 min at 56 °C, subsequently alkylated using Iodoacetic acid (IAA, 100 mM IAA diluted in 100 nM DTT and 100 mM NH_4HCO_3) and finally digested with trypsin initially for 4 h and then overnight at 37 °C. Next, each sample was reconstituted in trifluoracetic acid (TFA, 20%), then added to a column with a hydrophilic-lipophilic package equilibrated in water and subsequently eluted in a gradient of TFA/ACN (acetonitrile) with increasing concentrations of ACN.

Proteomics analysis using liquid chromatography-mass spectrometry (LC-MS/MS)

The digested protein samples were analyzed using the Orbitrap Fusion Lumos Tribid mass spectrometer and Nano ACQUITY with the HPLC system to obtain initial high mass accuracy survey MS/MS data for identification of the peptides present in the samples. C18 columns were used to separate peptides from the digested proteins.

Protein identification was determined using the UniProtKB database, which contained all proteins from mice and validated in PeptideProphet and ProteinProphet. Data were subjected to ontology and pathway analysis using protein analysis with the evolutionary relationships tool (PANTHER, http://www.pantherdb.org) and gene ontology algorithms (DAVID Bioinformatic Database 6.8, https://david.ncifcrf.gov/home.jsp). Venn diagrams were designed with the data (http://www.interactivenn.net/). Identified proteins were classified based on biological processes and molecular function categories.

Statistical analysis

Results were analyzed in GraphPad Prism 7.0 (San Diego, CA) using Kruskal-Wallis followed by Dunns post-test. Data were averaged from three independent experiments and are shown as the mean ± SEM. A value of $p < 0.05$ was considered statistically significant.

Results

Caveolin-1 phosphorylation on tyrosine-14 in murine melanoma cells does not affect EV release, size or morphology

B16F10 is a metastatic murine melanoma cell line that displays low endogenous levels of CAV1 [14]. Therefore, in order to evaluate the role of CAV1, these cells were stably transfected either with an empty pLacIOP plasmid [B16F10(Mock)] or a pLacIOP plasmid with sequences encoding either wild-type CAV1 [B16F10(CAV1)] or mutant CAV1 expressing the phosphomimetic [B16F10 (CAV1/Y14E)] or the phospho-null [B16F10 (CAV1/Y14F)] version of Y14, as previously described by our group [13]. EVs were isolated from the supernatants of these cells via ultracentrifugation and are referred to accordingly as EV Mock, EV CAV1, EV CAV1/Y14E and EV CAV1/Y14F. In terms of specific EV features, nanoparticle tracking analysis (NTA) revealed an EV size distribution ranging from 90 to 300 nm in diameter (Fig. 1A) with concentrations of 1.45×10^{11}, 1.73×10^{11}, 1.60×10^{11} and 1.69×10^{11} vesicles per milliliter, respectively (Fig. 1B). When segregating these particles into different size ranges, we observed that approximately 80% could be categorized as small vesicles (< 200 nm) (Fig. 1C), with a mode between 130 and 140 nm in the acquisition diameter (Fig. 1D) and a mean diameter of 160–170 nm (Fig. 1E). Transmission electron microscopy (Fig. 1F) confirmed the spherical shape of the different EV populations and revealed an approximate size that agrees with the data obtained by NTA.

EVs were also characterized by western blotting, where proteins, frequently used as EV markers, such as ALIX, TSG101 and CD81, were detected in all EV preparations. The absence of β-actin was also confirmed, indicating that these vesicle preparations were free of cell debris. Furthermore, the presence of CAV1 was detected in EVs isolated from all cell lines expressing CAV1; however, it is noteworthy that in CAV1(Y14F) vesicles, CAV1 levels were roughly 50% lower than in CAV1(Y14E) or CAV1 wild-type EVs, considering that the same amounts of total protein were loaded per lane (Fig. 1G).

B16F10(CAV1) and (CAV1/Y14E), but not (CAV1/Y14F) EVs promote migration, as well as invasion of B16F10(Mock) cells

The role of Y14 phosphorylation on CAV1 in EVs was also evaluated in terms of the effects such vesicles had in recipient cells. To this end, B16F10(Mock) cells were incubated with (Mock), (CAV1), (CAV1/Y14E) and (CAV1/Y14F) EVs for 24 h and subsequently evaluated in migration and invasion assays. The results obtained showed that (CAV1) and (CAV1/Y14E) EVs both induced 3D migration (Fig. 2A and C) and invasion (Fig. 2B and D) of recipient cells by at least two- to three-fold when compared to the effect of (Mock) and (CAV1/Y14F) EVs. As a control, the uptake of labeled EVs by cells was evaluated and no significant differences in the internalization of the different EV populations were detectable after 24 h (Supplementary Fig. S1). Thus, the variations observed in

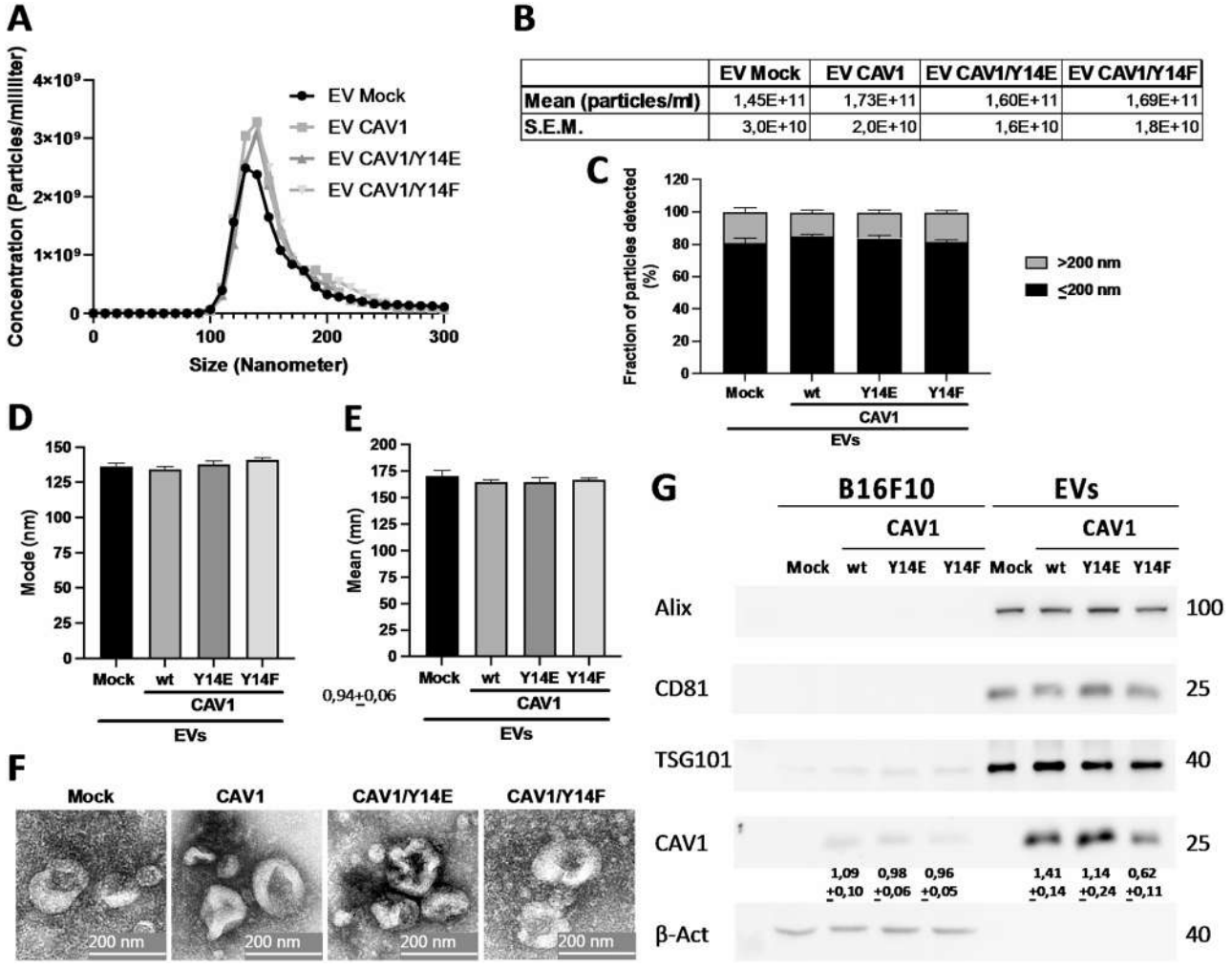

	EV Mock	EV CAV1	EV CAV1/Y14E	EV CAV1/Y14F
Mean (particles/ml)	1,45E+11	1,73E+11	1,60E+11	1,69E+11
S.E.M.	3,0E+10	2,0E+10	1,6E+10	1,8E+10

Fig. 1 B16F10 metastatic sublines release extracellular vesicles independent of CAV1 expression. **A**) Distribution of the detected EVs shows similar heterogeneity for EVs from B16F10(Mock), (CAV1), (CAV1/Y14E) and (CAV1/Y14F) expressing cells. **B**) EV heterogeneity indicated as the percentage of vesicles displaying a size > 200 nm and ≤ 200 nm in each sample. **C**) Concentration of EVs from each sample. **D**) Mean and **E**) Mode of the EVs analyzed. **F**) Morphology and approximate size of each EV sample is shown by transmission electron microscopy. Values shown in the graphs are the mean +/- SEM ($n = 3$). **G**) Representative western blots of cell extracts (50 µg) and EVs (15 µg) from B16F10(Mock), (CAV1), (CAV1/Y14E) and (CAV1/Y14F) contained the EV markers Alix, TSG101 and CD81. EVs did not contain β-actin. Quantification of EV CAV1 levels in CAV1, CAV1/Y14E and CAV1/Y14F EVs averaged from three different experiments are shown below the respective lanes (mean +/- SEM, $n = 3$)

the responses of recipient cells were not attributable to differences in EV uptake.

Proteins identified in EV preparations from B16F10 (CAV1) and (CAV1/Y14E) cells were linked to signaling pathways associated with cell adhesion and migration

A more exhaustive characterization of the protein content of Mock, CAV1, CAV1/Y14E and CAV1/Y14F EVs was carried out by shotgun mass spectrometry analysis. A total of 124 proteins were identified in Mock EVs, 224 proteins in CAV1 EVs, 295 proteins in CAV1/Y14E EVs and 210 proteins in CAV1/Y14F EVs. A comparative analysis (see Venn diagram) revealed that 115 proteins were common to all the different EV populations. In addition, one unique protein was identified in Mock EVs, 12 in CAV1 EVs, 12 in CAV1/Y14F EVs and 80 in CAV1/Y14E EV samples (Fig. 3A). Note that a complete list of all peptides detected by proteomics analysis in the different EV populations can be found in the supplementary data file (Proteomics EV analysis- raw data-Huilcaman et al.) that has been included.

The proteomic profiles were analyzed in order to obtain information regarding the groups of proteins that were enriched in each of the EV populations. A gene ontology enrichment analysis was performed using DAVID Bioinformatics Resources by classifying the different protein groups in each of the vesicle populations. Results showed that for both CAV1 and CAV1/Y14E EVs the abundance of proteins involved in the biological processes migration

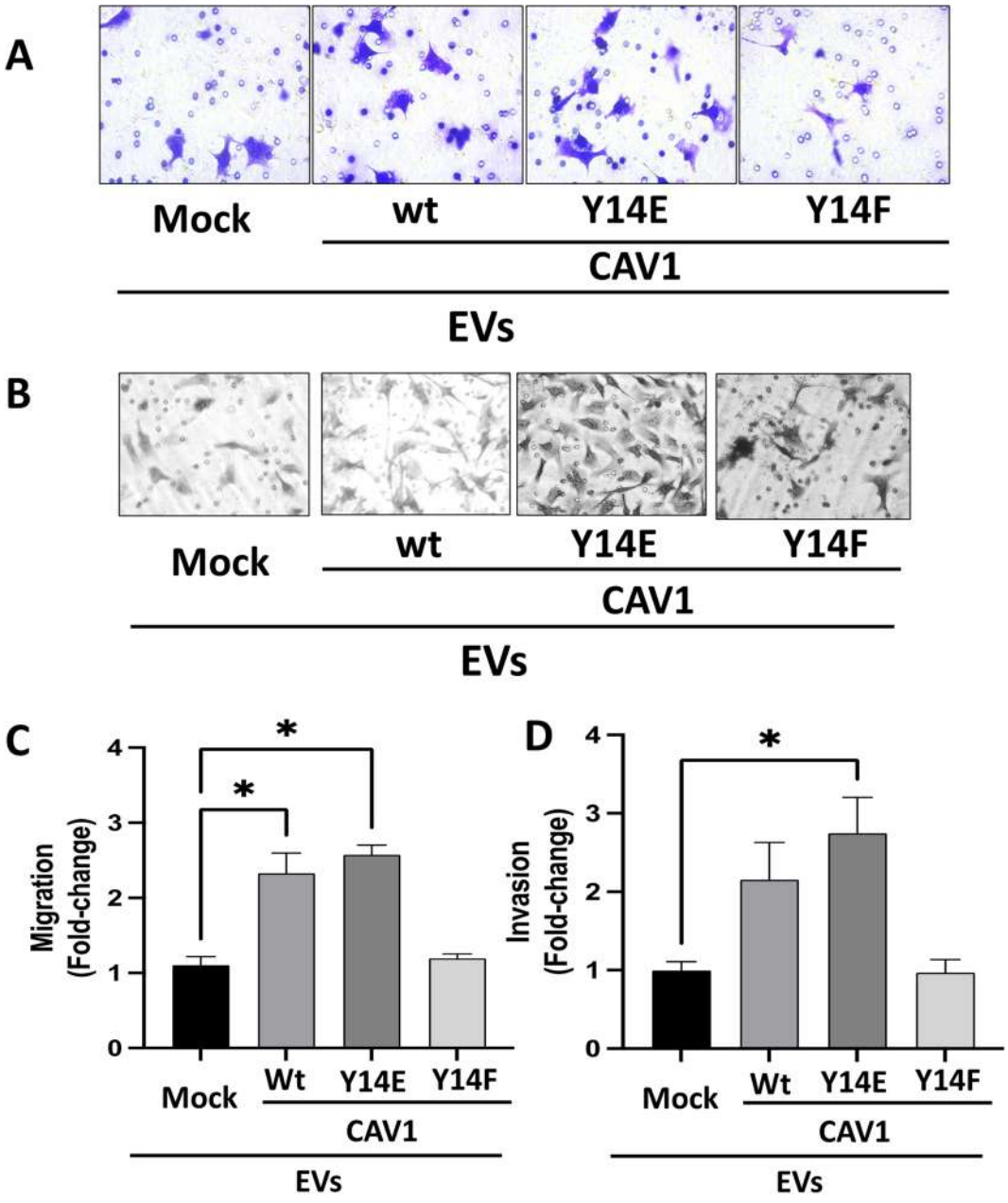

Fig. 2 Extracellular vesicles derived from the metastatic melanoma cancer cell lines B16F10 (CAV1) and (CAV1/Y14E) promote migration and invasion in B16F10 (Mock) cells. Migration (**A**, **C**) and invasion (**B**, **D**) assays were performed with metastatic B16F10 (Mock) cells pre-incubated for 24 h with 10 µg of the indicated EV samples. **A**) Cells (2×10^5) were allowed to migrate for 2 h and subsequently detected after fixation and staining of the lower side of the membrane with 0.1% crystal violet in 2% ethanol. (WT): CAV1-containing EVs. **B**) Cells (2×10^5) were seeded onto matrigel inserts, allowed to invade for 22 h and subsequently detected after fixation on the lower side of the membrane by staining with 0.1% Toluidine Blue. Values obtained were normalized to the average value obtained for Mock cells without treatment (**C** and **D**). Data in the graphs are the mean +/- SEM ($n=3$)

and adhesion were generally higher than in Mock and CAV1/Y14F EVs (Fig. 3B).

β3 integrin is transferred to B16F10 mock cells via uptake of B16F10(CAV1/Y14E) EVs

In cell migration and invasion, tumor cells begin to adhere and advance through matrices depending on the tissue they invade and one of the key groups of proteins that mediate these processes are integrins. In the case of melanoma development, particularly the upregulation of β1 and β3 integrins in the vertical growth phase is associated with metastasis [32, 33]. Moreover, β3 integrin expressing melanomas tend to metastasize preferentially to the lung [34]. In the proteomics analysis, we noted a considerable enrichment of some integrins in CAV1 and CAV1/Y14E EVs compared to CAV1/Y14F or Mock EVs

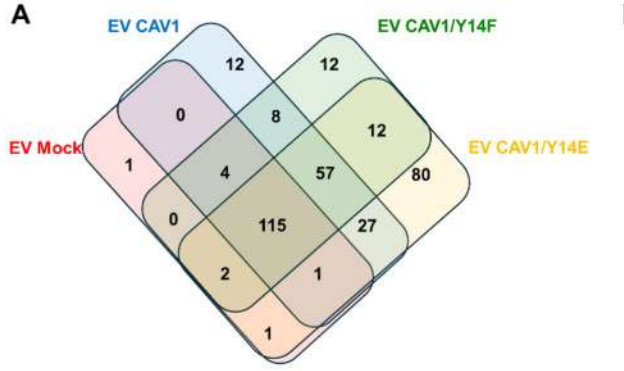

B

EV sample	Biological Process (GO)	Count	%	p-value
EV (Mock)	Protein transport	15	11,8	3,40E-05
	Signal transduction	15	11,8	3,70E-02
	Cell division	13	10,2	5,50E-06
	Cell adhesion	13	10,2	2,90E-04
	Cell cycle	12	9,4	2,10E-03
	Cell migration	11	8,7	1,70E-05
	Protein localization to plasma membrane	10	7,9	9,50E-07
	Endocytosis	10	7,9	3,2E-06

EV sample	Biological Process (GO)	Count	%	p-value
EV (CAV1)	Protein transport	29	12,8	5,10E-10
	Signal transduction	26	11,5	8,50E-03
	Cell adhesion	22	9,7	3,20E-06
	Cell migration	20	8,8	1,30E-09
	Regulation of cell shape	17	7,5	1,80E-11
	Cell division	17	7,5	8,90E-06
	Cell cycle	17	7,5	2,30E-03
	Translation	16	7	2,20E-06

EV sample	Biological Process (GO)	Count	%	p-value
EV (CAV1/Y14E)	Protein transport	35	11,7	4,50E-11
	Signal transduction	34	11,4	2,10E-03
	Cell adhesion	32	10,7	6,90E-10
	Cell migration	24	8,1	9,00E-11
	Regulation of cell shape	20	6,7	9,80E-13
	Angiogenesis	20	6,7	2,90E-08
	Cell division	19	6,4	1,80E-05
	Negative regulation of apoptotic process	19	6,4	6,60E-03

EV sample	Biological Process (GO)	Count	%	p-value
EV (CAV1/Y14F)	Protein transport	27	12,7	2,50E-09
	Signal transduction	24	11,3	1,40E-02
	Cell division	19	8,9	1,70E-07
	Cell cycle	18	8,5	4,30E-04
	Cell migration	16	7,5	6,60E-07
	Cell adhesion	16	7,5	1,40E-03
	Regulation of cell shape	15	7	8,40E-10
	Protein localization to plasma membrane	14	6,6	2,40E-08

Fig. 3 Extracellular vesicle proteins from B16F10(CAV1), (CAV1/Y14E) cells are involved in biological processes associated with protein transport, signal transduction, cell adhesion and cell migration. **A**) Venn diagram of the proteins identified in EVs from B16F10(Mock), (CAV1), (CAV1/Y14E) and (CAV1/Y14F) cells. **B**) Gene ontology protein enrichment analysis of EVs from (Mock), (CAV1), (CAV1/Y14E) and (CAV1/Y14F) cells showing the number of proteins detected in each category (Biological process)

(Fig. 4A). Interestingly, an increase in the presence of alphaV and β3 integrin was particularly notable in CAV1 and CAV1/Y14E EVs when compared to CAV1/Y14F EVs (Fig. 4B). This was also corroborated by western blotting, although staining for this integrin was weak in the EV fractions (Supplementary Fig. S2). For these reasons, we focused our subsequent analysis primarily on evaluating the possible role of β3 integrin in EVs.

To provide further evidence that β3 integrin transfer by EVs to recipient cells occurs, B16F10(Mock) cells were treated with EVs derived from CAV1/Y14E cells for 24 h and subsequently, total and surface integrin content was evaluated by western blotting and flow cytometry, respectively. In these experiments, we focused on the use of CAV1/Y14E EVs because in the functional assays, these vesicles tended to trigger slightly higher effects in recipient B16F10(Mock) cells. The incubation with CAV1/Y14E EVs did not lead to readily visible changes in total integrin levels, although a trend was noticeable (Fig. 4C) but did favor increased surface expression of the β3 integrin in these recipient cells (Fig. 4D). Thus, the CAV1/Y14E EVs serve as vectors for integrin transfer to recipient B16F10(Mock) cells and specifically result in increased presence of β3 integrin, which is implicated in promoting melanoma metastasis to the lung.

EVs from B16F10(CAV1/Y14E) promote metastasis and this process is blocked by using anti- AVβ3 integrin antibodies

As a next step, we evaluated whether EV pre-treatment with integrin-blocking antibodies would preclude the biological effects of EVs in recipient cells. To this end, we compared the effects of antibodies against β3 and β1 integrins. As indicated previously, upregulation of these integrins in the vertical phase is associated with melanoma metastasis. Only treatment with antibodies against αvβ3 significantly reduced the ability of CAV1/Y14E EVs to promote B16F10(Mock) cell migration, while pre-treatment with the antibodies against β1 integrin, which is abundantly present in EVs (see Fig. 4A), had no effect in this assay (Fig. 5A, C). Somewhat surprisingly, however, both antibodies reduced invasion to a similar extent (Fig. 5B, D).

Finally, to evaluate the effect of these vesicles in an in vivo metastasis model, B16F10(Mock) cells previously treated with 1mM IPTG and B16F10(CAV1), (CAV1/Y14E) or (CAV1/Y14F) EVs were injected intravenously into syngeneic C57BL/6 mice (Fig. 6A). The treatment with either (CAV1) or (CAV1/Y14E) EVs increased the lung tumor mass roughly 2-fold and over 5-fold, respectively, compared to the extent of metastasis observed with untreated B16F10(Mock) cells. Importantly, the lung tumor mass in animals inoculated with B16F10(Mock) cells previously treated with (CAV1/Y14F) EVs was similar to that observed for untreated B16F10(Mock) cells (Fig. 6B). Finally, the pre-treatment of (CAV1/Y14E) EVs with a blocking antibody against αVβ3 integrin completely prevented their ability to promote lung metastasis, while for the treatment with the anti-IgG control antibody, no significant reduction in the effects of (CAV1/Y14E) EVs was detected (Fig. 6C). Alternatively, treatment with the anti-β1 integrin antibody did reduce,

A

	PEPTIDES DETECTED			
	EV MOCK	EV CAV1	EV CAV1/Y14E	EV CAV1/Y14F
Integrin alpha-4	25,0	28,7	41,3	34,3
Integrin alpha-5	0,0	5,0	13,0	2,0
Integrin alpha-6	11,3	16,7	19,7	11,7
Integrin alpha-9	0,0	0,0	2,3	0,0
Integrin alpha-V	2,3	10,3	13,0	2,7
Integrin beta-1	25,7	28,0	41,3	29,3
Integrin beta-3	0,0	4,3	7,7	0,0
Integrin beta-5	0,0	3,7	3,0	0,0

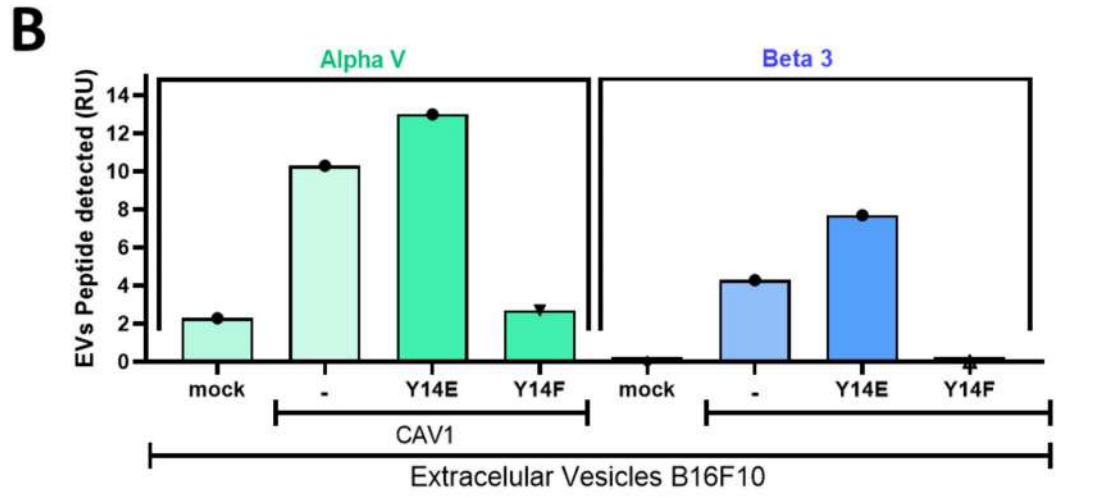

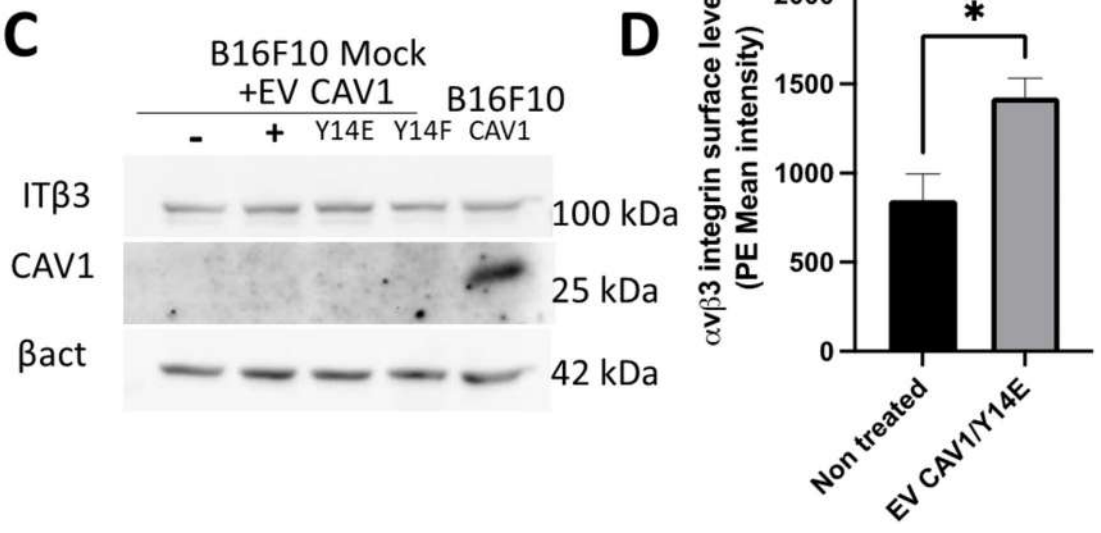

Fig. 4 B16F10(CAV1) and (CAV1/Y14E) EVs display preferential loading with αVβ3 integrin peptide cargos that are transferred to recipient cells. **A**) Table showing the integrins that were found to be enriched in EVs from B16F10 (CAV1) and (CAV1/Y14E) cells. **(B)** Representative graphical illustration of the relative preference for Integrin αV and β3 peptides detected in EVs. **(C)** Western blot analysis of B16F10(Mock) cells showing the levels of β3 integrin after incubation with EVs from Mock (-), CAV1 (+), CAV1(Y14E) or CAV1(Y14F) cells. As a control, integrin β3 levels in B16F10 (CAV1) cells are shown. **(D)** B16F10 (Mock) cells were treated with or without 10 µg of CAV1/Y14E EVs for 24 h. The values in the graph are the mean fluorescence intensities of αVβ3 Integrin/Phycoerythrin. Values represent mean +/- SEM ($n = 3$)

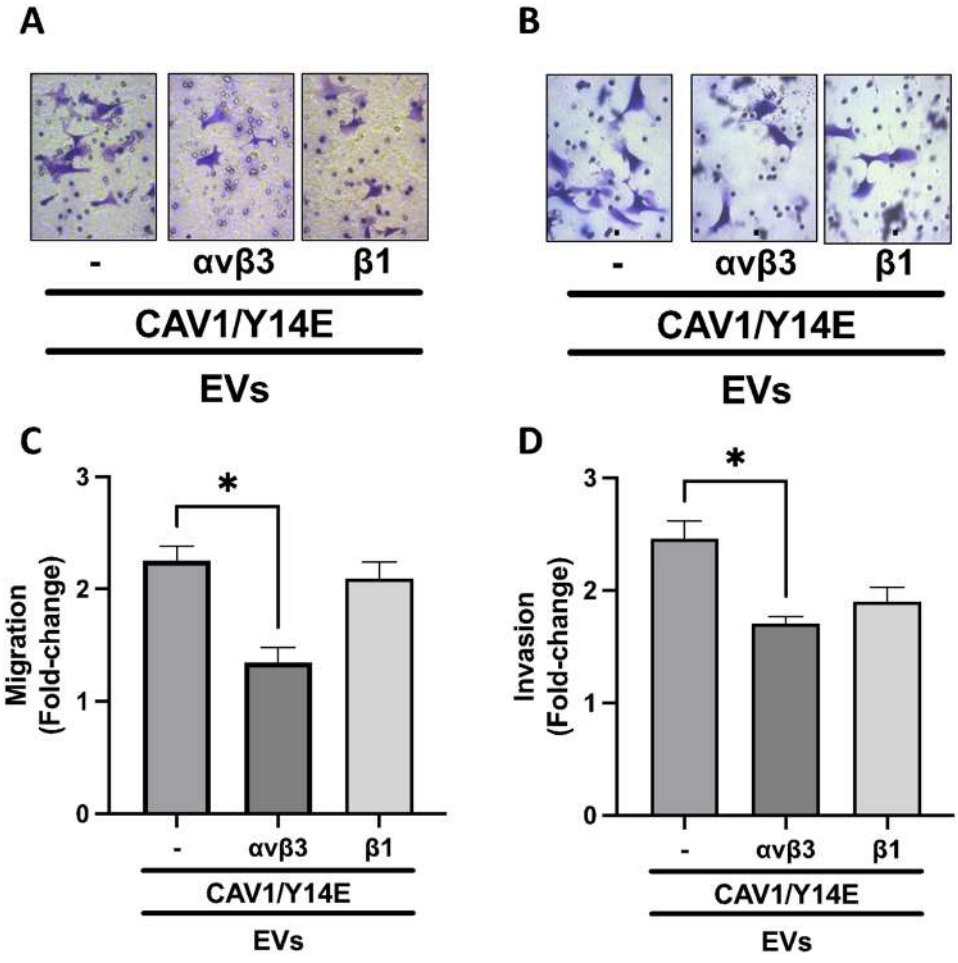

Fig. 5 EV integrins promote migration and invasion of recipient melanoma cells. EVs (10 µg) were pretreated with anti-αvβ3 or anti-β1 integrin antibodies for 30 min at 37 °C. The B16F10(Mock) cells were then incubated with pre-treated EVs at 37 °C for 24 h. **A**) EV-treated cells (2×10^5) were added to the transwell inserts, allowed to migrate for 2 h and subsequently detected after fixation on the lower side of the membrane by staining with 0.1% crystal violet in 2% ethanol. **B**) EV-treated cells (2×10^5) were seeded onto the matrigel inserts, allowed to migrate for 22 h and consequently detected after fixation on the lower side of the membrane by staining with 0.1% Toluidine Blue. Values obtained were normalized to those obtained for parental cells without treatment (**C** and **D**). Data in the graphs represent mean +/- SEM ($n=3$)

albeit to a lesser extent, the ability of (CAV1/Y14E) EVs to promote B16F10(Mock) cell metastasis to the lung.

Discussion

This study sought to evaluate the relevance of CAV1 and Y14 phosphorylation in determining the properties of EVs generated by the metastatic murine melanoma cell line, B16F10. In addition, we aimed to evaluate the biological effects that these EVs trigger in recipient cells with respect to migration, invasion and metastasis. B16F10 sublines were transfected with empty vector [B16F10(Mock)], or vector permitting the expression of wild-type CAV1 [B16F10(CAV1)], or CAV1 with the mutations Y14E [B16F10(CAV1/Y14E)] or Y14F [B16F10(CAV1/Y14F)] [13].

Subsequently, EVs were isolated from conditioned media of the B16F10 cells, expressing or not CAV1, CAV1(Y14/E) or CAV1(Y14F). Approximately 75–80% of the EVs were smaller in size than 200 nm, independent of the cell line used. These values are consistent with those reported in the literature to demonstrate the quality of the preparation obtained [21] and for the classification by size of the most abundant vesicles according to ISEV [23]. Western blot assays demonstrated that the EVs isolated contained proteins involved in their genesis. On the one hand, EVs contained elements of the ESCRT complex, such as ALIX and TSG101 proteins. In addition, EVs contained CD81, which is enriched in regions of the multivesicular body membrane similar to lipid rafts and constitutes a mechanism for loading cargo into extracellular vesicles that is independent of the ESCRT pathway [35]. Considering that CAV1 and CD81 are present in lipid rafts [36, 37] and implicated in endocytic processes [38], this suggests a potential role of CAV1 in the genesis and loading of EVs originating in the endocytic pathway.

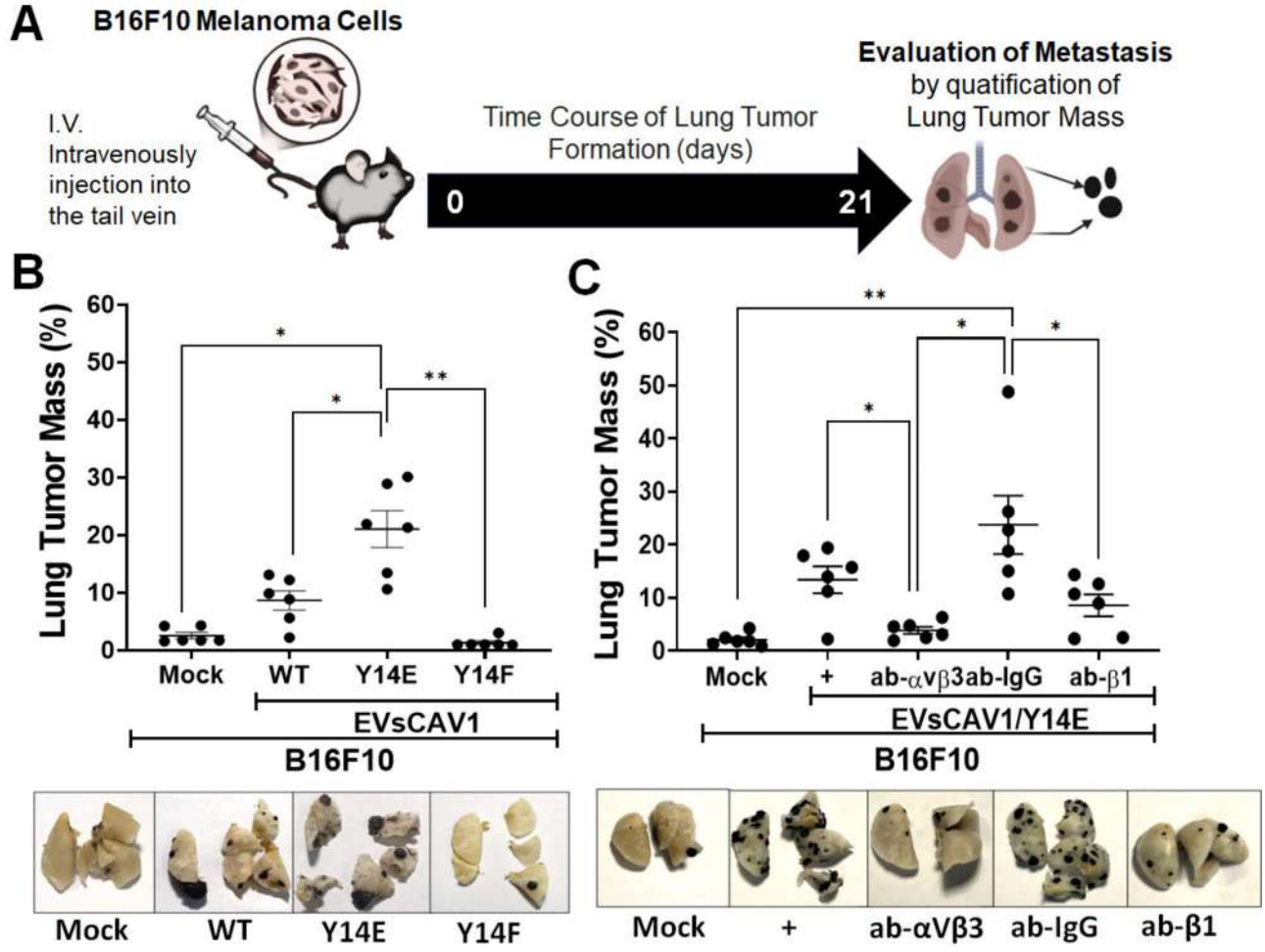

Fig. 6 EV integrins determine the ability of these vesicles to promote metastasis. **A)** C57BL/6 mice were injected intravenously into the tail vein with B16F10 cells (4 × 105) that were treated for 24 h in the presence of the EVs indicated. After 21 days mice were sacrificed and the complete lung, as well as metastatic tumor mass were determined. **B)** Average values for lung occupation by tumors in mice inoculated with B16F10(Mock) cells pre-treated with the indicated EVs. **C)** Average values for lung occupation by tumors in mice inoculated with B16F10(Mock) cells alone or B16F10(Mock) cells treated with either CAV1/Y14E EVs, or CAV1/Y14E EVs pretreated with either an anti-αVβ3 integrin antibody, an anti-IgG Isotype control antibody or with an anti-β1 integrin antibody. Values were normalized to those obtained for Mock cells without treatment. Data in the graphs represent mean +/- SEM (*n*=6). (T Test unpaired, multi-comparison Tukey. IC 95, * $p<0.05$, ** $p<0.01$)

In addition, EVs of CAV1 over-expressing cells contain CAV1. Previous studies in other metastatic lines, as well as in patients confirm the presence of CAV1 in small and large EVs of tumor cell origin [27, 29, 39, 40]. Moreover, western blot assays demonstrated that CAV1 phosphorylation on Y14 modulates the presence of CAV1 in EVs. Although CAV1 is present in B16F10 vesicles that express CAV1 and its mutants, it is interesting to note the decrease in CAV1 detected in the EVs derived from B16F10 cells expressing CAV1/Y14F. Thus, CAV1 phosphorylation on Y14 emerges as being relevant not only to the processes of migration, invasion and metastasis of cancer cells [12, 41], but also to the presence of CAV1 in EVs. Given our previous work showing that CAV1 regulates the protein composition of EVs [29], we anticipated that the EV protein cargos should also vary in function of the degree of CAV1 Y14 phosphorylation. Furthermore, CAV1 phosphorylation at this site promotes malignancy of the respective cancer cells (cell intrinsic effects), and this is reflected again in the biological effects of the EVs derived from such cells on recipient cells (cell extrinsic effects). That is, EVs from wild-type CAV1 and phosphomimetic CAV1(Y14E) expressing cells also promote migration and invasion of recipient cells, while EVs derived from cells over-expressing phospho-null CAV1(Y14F) were unable to do so.

Proteomics analysis of EV composition identified a unique profile of proteins present exclusively or highly enriched in CAV1 and CAV1(Y14E) EVs, as is the case for β3 and β5 integrins, which likely contribute to aggressiveness of recipient cells. This result is consistent with evidence in the literature showing that circulating EV β3

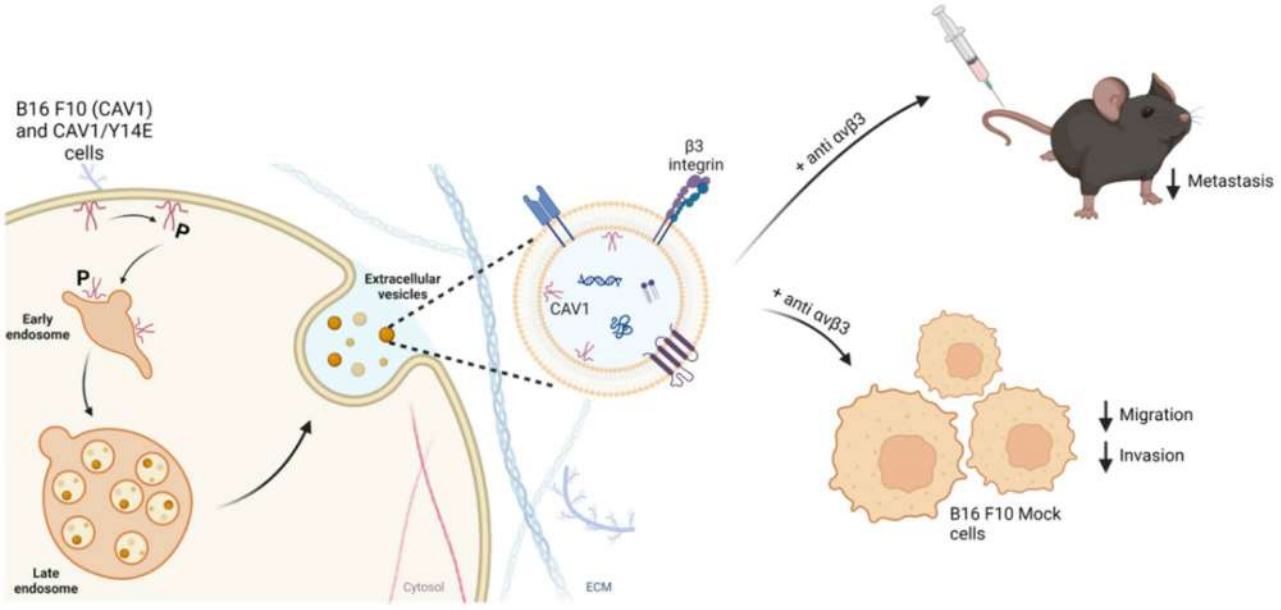

Fig. 7 Schematics showing that phosphorylation on tyrosine 14 in CAV1 is relevant to the recruitment of CAV1-specific cargo into EVs released by B16F10 cells overexpressing CAV1. This effect can be simulated by expression of the phosphomimetic form of this protein (CAV1/Y14E). In both cases, EVs were found to be enriched in cell adhesion proteins, such as β3 integrin. Interestingly, when EVs were previously incubated with αvβ3 blocking antibodies, these were unable to promote migration or invasion in recipient B16F10(Mock) cells in vitro or metastasis in vivo following tail vein injection of C57BL/6 mice

integrin levels correlate with poor survival and increased incidence of intracranial metastasis in humans [42]. Moreover, β5 integrin together with its pair, the αV integrin, bind to components of the extracellular matrix, like fibronectin and vitronectin, both of relevance in cancer metastasis [43]. Furthermore, the interaction between integrins on EVs and fibronectin or vitronectin on the surface of recipient cells appears to be important for EV uptake [44]. In addition, αV and β1 integrin subunits are enriched in EVs of highly metastatic origin in mice and humans. Moreover, inhibition of the αVβ1 integrin complex leads to a reduction in the binding of EVs to fibronectin, suggesting a decrease in EV retention by the extracellular matrix and thereby a reduction in the metastatic potential of breast cancer cells [45]. Finally, blocking αVβ3 integrin impairs the uptake of EVs by recipient cells [46].

Taken together, the aforementioned observations from the literature all pointed towards a potentially important role for integrins on the surface of EVs as being crucial to their ability to elicit responses in recipient cells.

In the case of melanoma development, particularly the upregulation of β1 and β3 integrins in the vertical growth phase is associated with metastasis. Moreover, β3 integrin expressing melanomas tend to metastasize preferentially to the lung [34]. Considering this available data and our proteomics analysis, we focused on evaluating particularly whether these two integrins may be important in the transfer of information from more aggressive to less aggressive melanoma cells. For this analysis, we used blocking antibodies specific to αVβ3 integrin because αV is the only α-subunit that can pair with β3 in melanoma cells, while β1 potentially pairs with many of the α-subunits detected in the EVs. Also, we concentrated on the use of EVs from CAV1(Y14E) expressing cells and observed that antibodies blocking αVβ3 integrin reduced substantially CAV1/Y14E EV-induced migration, invasion and metastasis of recipient B16F10(Mock) cells, while this was only partially the case for β1 integrin-blocking antibodies. This reduced effect in vivo is likely linked to the observation that the antibody partially blocked EV-stimulated invasion but not migration (see Fig. 5). In addition, β1 integrin has been described to play a crucial role in promoting cancer progression and metastasis through its involvement in exosome-mediated communication between cancer cells and their microenvironment [47, 48]. In this regard, results have shown that exosomes containing β1 integrin upregulate fibroblast proteins involved specifically in cell adhesion (α2/α6/αv, β1/β4/β5, EGFR, CRK), cytoskeleton regulation (RAC1, ARF1, ARPC3, CYFIP1, NCKAP1, ICAM1, and ERM complex), and signaling pathways (MAPK, Rap1, RAC1, and Ras), leading to the remodeling of the extracellular matrix (ECM) and the creation of pre-metastatic niches [47]. Thus, the aforementioned data may support the notion that β1integrin has a distinctive role in cancer when compared to β3 integrin function in this disease.

In conclusion, our results demonstrate for the first time that CAV1 phosphorylation on Y14 is relevant to the inclusion of CAV1 and select cargo proteins within EVs in cancer cells. In this sense, EVs derived from cancer cells overexpressing wild-type and phosphomimetic CAV1 contain proteins implicated in adhesion, migration, invasion and metastasis, such as β3 integrin. Moreover, blocking αVβ3 integrin reduced the metastatic potential of recipient cells, thereby suggesting that these proteins are relevant in the aggressiveness conferred by EVs from CAV1-expressing melanoma cells. Blocking integrin function in EVs is therefore crucial in cancer due to the fact that it disrupts the vesicles' role in promoting metastasis, tumor-stroma communication and extracellular matrix remodelling [48]. This interference can reduce cancer cell invasion, inhibit the formation of pre-metastatic niches, and potentially overcome therapeutic resistance, making it a significant target for limiting cancer progression. Interestingly, in this context, we have previously shown that treatment of CAV1-expressing B16F10 melanoma cells with src-family kinase inhibitors prior to injection into the tail vein of C57BL/6 mice precludes CAV-1-enhanced lung metastasis [13]. Thus, it is intriguing to speculate that treatment of CAV1-expressing cells with these inhibitors might not only reduce metastasis by the same cells (effect in cis), but also preclude the genesis of EVs that promote metastasis (effect in trans) as is observed for the EVs derived from CAV1(Y14F) cells (Fig. 6B). In this perspective, it is interesting to speculate further that such EVs from inhibitor-treated cells may serve therapeutical purposes to prevent metastasis where CAV1 is implicated (Fig. 7).

Supplementary Information

The online version contains supplementary material available at https://doi.org/10.1186/s12964-025-02131-0.

Supplementary Material 1

Acknowledgements

This work was possible thanks to the use of the Nanosight NS300 equipment (FONDEQUIP EQM160157). We thank Cecilia Zuñiga and Herve Camus of the CEMC facility for their technical support relating to use of the ultracentrifuge (Sorvall WX + 100). The authors thank Ruth Mora for her valuable veterinary assistance in our animal facility. The authors also thank A.C. for the use of her paid account to make the figures created with BioRender.com.

Author contributions

Huilcaman R: experimental, scientific discussion and prepared the manuscriptCampos A: experimental, scientific discussion and prepared the manuscriptOrellana P: experimental assays an in vivo model Simon L: experimental, scientific discussionVaras-Godoy M: In silico analysis and scientific discussion Grünenwald F: experimental assays and In silico analysis Baohai Shao: experimental assaysJay Heinecke: experimental assays and scientific discussion Lobos-Gonzalez L: experimental discussion, support, supervision, and prepared and reviewed the manuscriptLeyton L: corresponding author, experimental discussion and support and prepared and reviewed the manuscriptQuest A.F.G: corresponding author, experimental discussion and support and prepared and reviewed the manuscript.

Funding

This work was supported by FONDECYT grants 1210644 (A.F.G.Q.), 1200836, 1240888 (L.L.), 1211223 (L.L.-G.), 1230983 (M.V.G.), FONDAP grants 15130011 and 1523A0008 (A.F.G.Q., L.L., L.L.-G., M.V.G.), ANID/BASAL/FB210008 (M.V.G.), ANID postdoctoral fellowship award Becas Chile (A.C.), ANID PhD fellowship awards 21130102 (AC), 21161246 (R.H.).

Data availability

Additional datasets showing all the results obtained by mass spectrometry analysis of the different vesicle populations are available.

Declarations

Competing interests

The authors declare no competing interests.

Author details

[1]Cellular Communication Laboratory, Center for Studies on Exercise, Metabolism and Cancer (CEMC), Institute of Biomedical Sciences (ICBM), Faculty of Medicine, University of Chile, Santiago, Chile
[2]Advanced Center for Chronic Diseases (ACCDiS), Faculty of Medicine, University of Chile, Santiago, Chile
[3]Nutrition and Dietetic School, Universidad Finis Terrae, Santiago, Chile
[4]Centro de Biología Celular y Biomedicina (CEBICEM), Facultad de Medicina y Ciencia, Universidad San Sebastián, Providencia, Santiago 7510156, Chile
[5]Centro Científico y Tecnológico de Excelencia Ciencia & Vida, Fundación Ciencia & Vida, Huechuraba, Santiago 8580702, Chile
[6]Laboratory of Reproductive Biology, Center for Biomedical Research, Faculty of Medicine, Universidad de Los Andes, Santiago, Chile
[7]Division of Metabolism, Endocrinology and Nutrition, University of Washington, Seattle, WA 98195- 8055, USA
[8]Cancer Research UK Scotland Institute, Garscube Estate. Switchback Road, Bearsden, Glasgow G61 1BD, UK
[9]Facultad de Ciencias de la Salud, Escuela de Tecnología Médica, Universidad Bernardo OHiggins, General Gana 1702, Santiago 8370854, Chile

Received: 19 November 2024 / Accepted: 26 February 2025
Published online: 17 March 2025

References

1. World Health Organization. World Health Organization. 2021 [cited 2025 Jan 9]. Cardiovascular diseases (CVDs). Available from: https://www.who.int/news-room/fact-sheets/detail/cardiovascular-diseases-(cvds).
2. Sung H, Ferlay J, Siegel RL, Laversanne M, Soerjomataram I, Jemal A, et al. Global Cancer statistics 2020: GLOBOCAN estimates of incidence and mortality worldwide for 36 cancers in 185 countries. CA Cancer J Clin. 2021;71(3):209–49.
3. Matthews NH, Li WQ, Qureshi AA, Weinstock MA, Cho E. Epidemiology of melanoma. Cutaneous melanoma: etiology and therapy. Codon; 2017. pp. 3–22.
4. Leiter U, Keim U, Garbe C. In. Epidemiology of skin cancer: update 2019. 2020. pp. 123–39.
5. Nguyen DX, Bos PD, Massagué J. Metastasis: from dissemination to organ-specific colonization. Nat Rev Cancer. 2009;9(4):274–84.
6. Geho DH, Bandle RW, Clair T, Liotta LA. Physiological mechanisms of Tumor-Cell invasion and migration. Physiology. 2005;20(3):194–200.
7. Nunez-Wehinger S, Ortiz RJ, Diaz N, Diaz J, Lobos-Gonzalez L, Quest AFG. Caveolin-1 in cell migration and metastasis. Curr Mol Med. 2014;14(2):255–74.
8. Belkot K, Bubka M, Litynska A. Expression of Caveolin-1 in human cutaneous and uveal melanoma cells. Folia Biol (Praha). 2016;64(3):145–51.
9. Yang G, Truong LD, Timme TL, Ren C, Wheeler TM, Park SH, et al. Elevated expression of Caveolin is associated with prostate and breast cancer. Clin Cancer Res. 1998;4(8):1873–80.
10. Díaz J, Mendoza P, Ortiz R, Díaz N, Leyton L, Stupack D, et al. Rab5 is required in metastatic cancer cells for Caveolin-1-enhanced Rac1 activation, migration and invasion. J Cell Sci. 2014;127(Pt 11):2401–6.

11. Díaz J, Mendoza P, Silva P, Quest AF, Torres VA. A novel caveolin-1/p85α/Rab5/Tiam1/Rac1 signaling axis in tumor cell migration and invasion. Commun Integr Biol. 2014;7(5).
12. Lobos-González L, Aguilar L, Diaz J, Diaz N, Urra H, Torres VA, et al. E-cadherin determines Caveolin-1 tumor suppression or metastasis enhancing function in melanoma cells. Pigment Cell Melanoma Res. 2013;26(4):555–70.
13. Ortiz R, Díaz J, Díaz N, Lobos-Gonzalez L, Cárdenas A, Contreras P, et al. Extracellular matrix-specific Caveolin-1 phosphorylation on tyrosine 14 is linked to augmented melanoma metastasis but not tumorigenesis. Oncotarget. 2016;7(26):40571–93.
14. Urra H, Torres VA, Ortiz RJ, Lobos L, Díaz MI, Díaz N, et al. Caveolin-1-Enhanced motility and focal adhesion turnover require Tyrosine-14 but not accumulation to the Rear in metastatic Cancer cells. PLoS ONE. 2012;7(4):e33085.
15. Campos A, Burgos-Ravanal R, González M, Huilcaman R, Lobos González L, Quest A. Cell intrinsic and extrinsic mechanisms of Caveolin-1-Enhanced metastasis. Biomolecules. 2019;9(8):314.
16. Chambers AF, Groom AC, MacDonald IC. Dissemination and growth of cancer cells in metastatic sites. Nat Rev Cancer. 2002;2(8):563–72.
17. Sugarbaker PH. Metastatic inefficiency: the scientific basis for resection of liver metastases from colorectal cancer. J Surg Oncol. 1993;53(S3):158–60.
18. Wong CW, Lee A, Shientag L, Yu J, Dong Y, Kao G, et al. Apoptosis: an early event in metastatic inefficiency. Cancer Res. 2001;61(1):333–8.
19. Shao H, Im H, Castro CM, Breakefield X, Weissleder R, Lee H. New technologies for analysis of extracellular vesicles. Chem Rev. 2018;118(4):1917–50.
20. Möller A, Lobb RJ. The evolving translational potential of small extracellular vesicles in cancer. Nat Rev Cancer. 2020;20(12):697–709.
21. van Niel G, D'Angelo G, Raposo G. Shedding light on the cell biology of extracellular vesicles. Nat Rev Mol Cell Biol. 2018;19(4):213–28.
22. Zijlstra A, Di Vizio D. Size matters in nanoscale communication. Nat Cell Biol. 2018;20(3):228–30.
23. Théry C, Witwer KW, Aikawa E, Alcaraz MJ, Anderson JD, Andriantsitohaina R et al. Minimal information for studies of extracellular vesicles 2018 (MISEV2018): a position statement of the international society for extracellular vesicles and update of the MISEV2014 guidelines. J Extracell Vesicles. 2018;7(1).
24. Bartz R, Zhou J, Hsieh JT, Ying Y, Li W, Liu P. Caveolin-1 secreting LNCaP cells induce tumor growth of caveolin-1 negative LNCaP cellsin vivo. Int J Cancer. 2008;122(3):520–5.
25. Llorente A, de Marco MC, Alonso MA. Caveolin-1 and MAL are located on prostasomes secreted by the prostate cancer PC-3 cell line. J Cell Sci. 2004;117(22):5343–51.
26. Lazar I, Clement E, Ducoux-Petit M, Denat L, Soldan V, Dauvillier S, et al. Proteome characterization of melanoma exosomes reveals a specific signature for metastatic cell lines. Pigment Cell Melanoma Res. 2015;28(4):464–75.
27. Logozzi M, De Milito A, Lugini L, Borghi M, Calabrò L, Spada M, et al. High levels of exosomes expressing CD63 and Caveolin-1 in plasma of melanoma patients. PLoS ONE. 2009;4(4):e5219.
28. Lobos-Gonzalez L, Aguilar-Guzmán L, Fernandez JG, Muñoz N, Hossain M, Bieneck S, et al. Caveolin-1 is a risk factor for postsurgery metastasis in preclinical melanoma models. Melanoma Res. 2014;24(2):108–19.
29. Campos A, Salomon C, Bustos R, Díaz J, Martínez S, Silva V, et al. Caveolin-1-containing extracellular vesicles transport adhesion proteins and promote malignancy in breast cancer cell lines. Nanomedicine. 2018;13(20):2597–609.
30. Campos A, Burgos-Ravanal R, Lobos-González L, Huilcamán R, González MF, Díaz J, et al. Caveolin-1-Dependent Tenascin C inclusion in extracellular vesicles is required to promote breast Cancer cell malignancy. Nanomedicine. 2023;18(23):1651–68.
31. Díaz-Valdivia NI, Díaz J, Contreras P, Campos A, Rojas-Celis V, Burgos-Ravanal RA, et al. The non-receptor tyrosine phosphatase type 14 blocks caveolin-1-enhanced cancer cell metastasis. Oncogene. 2020;39(18):3693–709.
32. Van Belle PA, Elenitsas R, Satyamoorthy K, Wolfe JT, Guerry IVD, Schuchter L, et al. Progression-related expression of beta3 integrin in melanomas and nevi. Hum Pathol. 1999;30(5):562–7.
33. Hsu MY, Shih DT, Meier FE, Van Belle P, Hsu JY, Elder DE, et al. Adenoviral gene transfer of B3 integrin subunit induces conversion from radial to vertical growth phase in primary human melanoma. Am J Pathol. 1998;153(5):1435–42.
34. Huang R, Rofstad EK. Integrins as therapeutic targets in the organ-specific metastasis of human malignant melanoma. J Experimental Clin Cancer Res. 2018;37(1):92.
35. Perez-Hernandez D, Gutiérrez-Vázquez C, Jorge I, López-Martín S, Ursa A, Sánchez-Madrid F, et al. The intracellular interactome of Tetraspanin-enriched microdomains reveals their function as sorting machineries toward exosomes. J Biol Chem. 2013;288(17):11649–61.
36. Calzolari A, Raggi C, Deaglio S, Sposi NM, Stafsnes M, Fecchi K, et al. TfR2 localizes in lipid raft domains and is released in exosomes to activate signal transduction along the MAPK pathway. J Cell Sci. 2006;119(21):4486–98.
37. Viswanathan K, Verweij MC, John N, Malouli D, Früh K. Quantitative membrane proteomics reveals a role for tetraspanin enriched microdomains during entry of human cytomegalovirus. PLoS ONE. 2017;12(11):e0187899.
38. Pelkmans L, Bürli T, Zerial M, Helenius A. Caveolin-Stabilized membrane domains as multifunctional transport and sorting devices in endocytic membrane traffic. Cell. 2004;118(6):767–80.
39. Dorai T, Shah A, Summers F, Mathew R, Huang J, Hsieh T, et al. NRH:quinone oxidoreductase 2 (NQO2) and glutaminase (GLS) both play a role in large extracellular vesicles (LEV) formation in preclinical LNCaP-C4-2B prostate cancer model of progressive metastasis. Prostate. 2018;78(15):1181–95.
40. He M, Qin H, Poon TCW, Sze SC, Ding X, Co NN, et al. Hepatocellular carcinoma-derived exosomes promote motility of immortalized hepatocyte through transfer of oncogenic proteins and RNAs. Carcinogenesis. 2015;36(9):1008–18.
41. Ortiz R, Díaz J, Díaz-Valdivia N, Martínez S, Simón L, Contreras P, et al. Src-family kinase inhibitors block early steps of caveolin-1-enhanced lung metastasis by melanoma cells. Biochem Pharmacol. 2020;177:113941.
42. Chen GY, Cheng JCH, Chen YF, Yang JCH, Hsu FM. Circulating Exosomal integrin B3 is associated with intracranial failure and survival in lung Cancer patients receiving cranial irradiation for brain metastases: A prospective observational study. Cancers (Basel). 2021;13(3):380.
43. Desgrosellier JS, Cheresh DA. Integrins in cancer: biological implications and therapeutic opportunities. Nat Rev Cancer. 2010;10(1):9–22.
44. Hoshino A, Costa-Silva B, Shen TL, Rodrigues G, Hashimoto A, Tesic Mark M, et al. Tumour exosome integrins determine organotropic metastasis. Nature. 2015;527(7578):329–35.
45. Zhang DX, Dang XTT, Vu LT, Lim CMH, Yeo EYM, Lam BWS et al. αvβ1 integrin is enriched in extracellular vesicles of metastatic breast cancer cells: A mechanism mediated by galectin-3. J Extracell Vesicles. 2022;11(8).
46. Altei WF, Pachane BC, dos Santos PK, Ribeiro LNM, Sung BH, Weaver AM, et al. Inhibition of Avβ3 integrin impairs adhesion and uptake of tumor-derived small extracellular vesicles. Cell Communication Signal. 2020;18(1):158.
47. Su C, Mo J, Dong S, Liao Z, Zhang B, Zhu P. Integrinβ-1 in disorders and cancers: molecular mechanisms and therapeutic targets. Cell Communication Signal 2024. 2024;22(1):1.
48. Ji Q, Zhou L, Sui H, Yang L, Wu X, Song Q et al. Primary tumors release ITGBL1-rich extracellular vesicles to promote distal metastatic tumor growth through fibroblast-niche formation. Nature Communications 2020 11:1. 2020;11(1):1–18.

Publisher's note